Polymer 188 (2020) 122098

Contents lists available at ScienceDirect

Polymer

journal homepage: http://www.elsevier.com/locate/polymer

Recoverably and destructively deformed domain structures in elongation process of thermoplastic elastomer analyzed by graph theory

Hiroshi Morita [a,b,*], Ayano Miyamoto [a], Motoko Kotani [c]

[a] Research Center for Computational Design of Advanced Functional Materials (CD-FMat), National Institute of Advanced Industrial Science and Technology (AIST), Central 2-1, 1-1-1 Umezono, Tsukuba, Ibaraki, 305-8568, Japan
[b] Mathematics for Advanced Materials-OIL, National Institute of Advanced Industrial Science and Technology (AIST), Sendai, Miyagi, 980-8577, Japan
[c] Advanced Institute for Materials Research (AIMR), Tohoku University, Sendai, Miyagi, 980-8577, Japan

ARTICLE INFO

Keywords:
Thermoplastic elastomer
Coarse-grained molecular dynamics simulation
Triblock copolymer

ABSTRACT

Thermoplastic elastomer (TPE) by ABA triblock copolymer chains undergoes microphase separation with bridge and loop chains. TPE has a multi-scale structure containing both bridge chain networks and microphase separated structures in meso scale. In the uniaxial elongation process of TPE, coalescence and breaking of domains occur, and an irreversibly deformed structure forms at high strain. To understand the structural changes in an elongation, we performed coarse-grained molecular dynamics simulations of the elongation process of TPE and analyzed the changes of both the bridge chain network and domain structure by graph theory. Both the changes of the domain structures and recombination of bridge chains can be understood by the descriptors of each graph structure. Using the graph description, two types of structures can be found in the elongation process; recoverably and destructively deformed structures. The graph is one of the most useful mathematical descriptors to understand the topology of bridge chain network inside the structures of TPE in the elongation process, including fracture of domains with a microscopic chain conformation.

1. Introduction

Thermoplastic elastomer (TPE) [1] has attracted attention as a recyclable material, and if it is heated above the glass transition temperature, it can be molded again. Many studies of development of high functional TPEs and detailed analysis of these materials have been performed. ABA triblock copolymers are sometime used as the primary molecule of TPE, where the A and B species are hard and soft blocks connected by covalent bonds, respectively. At the mesoscale, microphase separated structures, such are spheres, cylinders, gyroids, and lamellar domain structures, form by self-assembly [2,3]. For a small fraction of the A block, the microphase separated structure is a body-centered cubic (BCC) sphere structure (Fig. 1(a)). A schematic diagram of the ABA domain is shown in Fig. 1(b), in which the spherical A domain is composed of A blocks and the B matrix domain constitutes the middle B block. Two types of ABA block copolymer conformations are found in this structure: bridge and loop chains. If two A blocks belong to the same A domain, the chain is called a loop chain. If two A blocks are in different A domains, the chain is called a bridge chain. These conformations have been investigated by theory [4], experiments [5,6], Monte Carlo simulations [7,8], and molecular dynamics simulations [9]. From the viewpoint of the higher order structure, it can be considered that the domain network forms as a "bridge chain network". In the expansion process, the domain structures deform and the distance between the domains on the elongation axis increases. As a consequence, some bridge chains expand and contribute to the mechanical stress during deformation.

For TPE, understanding of the structure and dynamics of bridge chains is very important. Many simulation studies of analysis of TPE materials have been reported. Structural analysis for microphase separation [10–12] has been performed by self consistent field (SCF) theory [13–16] and the mechanical properties [9,16–18] have been investigated by molecular dynamics simulations [19]. The bridge fraction has also been investigated by SCF theory [20], and the bridge fraction in the equilibrium structure is estimated to be almost 70%.

Aoyagi et al. [9] investigated elongation of TPE and analyzed the bridge fraction by coarse-grained molecular dynamics (CGMD) simulations. They constructed the initial structure based on the bead-spring

* Corresponding author. Research Center for Computational Design of Advanced Functional Materials (CD-FMat), National Institute of Advanced Industrial Science and Technology (AIST), Central 2-1, 1-1-1 Umezono, Tsukuba, Ibaraki, 305-8568, Japan.
E-mail address: h.morita@aist.go.jp (H. Morita).

https://doi.org/10.1016/j.polymer.2019.122098
Received 7 October 2019; Received in revised form 6 December 2019; Accepted 18 December 2019
Available online 18 December 2019

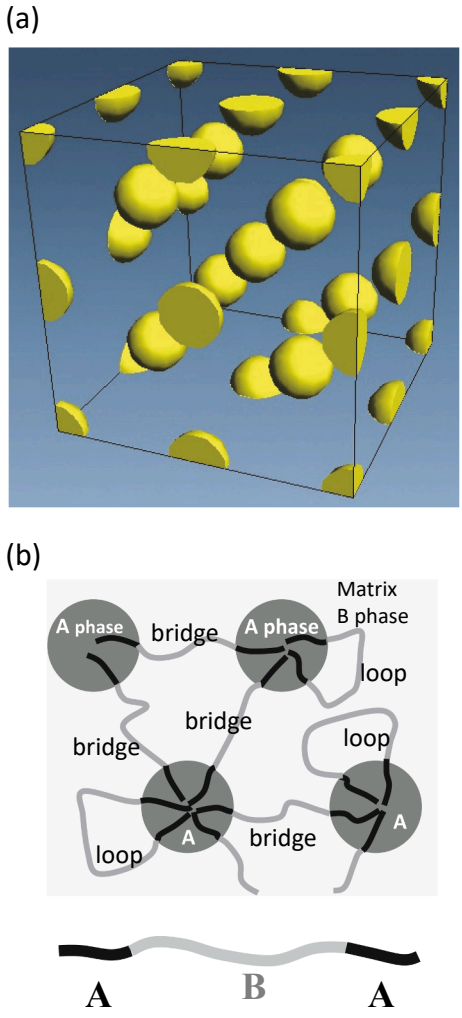

Fig. 1. (a) Model structure and (b) molecular structure of the ABA domain.

model using a density-biased Monte Carlo method [21] with the density field obtained by a SCF simulation and then performed a uniaxial elongation simulation. They found that the number of domains decreases until the strain becomes 2.0, and it then increases in the larger strain range. The bridge fraction decreases until strain of 2.5, and it then increases when the strain is larger than 2.5. They also found that many chains are pulled out of the domains and the domains are finally destroyed for strain of above 3.5. They analyzed cycle deformation of TPE by CGMD simulations with analysis of the number of domains and bridge fraction, and they found that recoverable cycle deformation occurs under small strain. If the recent data and topological analysis are applied to deformation of TPE, more detailed analysis of the deformation process of TPE can be performed and deformation of TPE can be understood in much more detail.

To understand the structural changes of TPE during elongation, analysis of the structure, including both the chain conformations and domain structures, is required. In other words, the multiscale structures during deformation with fracture of the domain need to be understood. To describe these multi-scale structures of TPE, we used graph theory [22], which is a discrete mathematics or information technique method to analyze complex networks. The "small world" problem is one of the successful applications of graph theory [23]. Recently, the topology of a special synthesized polymer chain has been represented by a graph [24,25]. If graph theory is applied to TPE, the structural information of both the bridge chains and domain structures can be simply represented.

Here, we used graph theory to describe both the molecular conformation and domain structure of TPE in the uniaxial elongation process. This descriptor includes information about not only the bridge chain network and its topology, which contributes to the mechanical stress, but also the domain structure, and we used this method to analyze deformation of TPE. In Section 2, we give an overview of the simulation method. In Section 3, the results of the CGMD simulations in the elongation process are discussed and the details of the graph for the BCC spherical phase separated structure by the ABA triblock copolymer are presented. In addition, the recoverably and destructively deformed structures are analyzed by the correlation among the quantities obtained by graph theory. In Section 4, we give the conclusions of the study.

2. Simulation method

To simulate mechanical extension of TPE by the ABA triblock copolymer, we used the bead-spring (BS) model of Kremer and Grest [19]. The polymer consists of N beads connected by the bonding potential,

$$U^{B}(\mathrm{r}) = U^{FENE}(\mathrm{r}) + U^{LJ}(\mathrm{r}) \ , \tag{1}$$

where r is the distance between the beads. $U^{FENE}(\mathrm{r})$ and $U^{LJ}(\mathrm{r})$ are given by

$$U^{FENE}(r) = \begin{cases} -\frac{1}{2}kR_0^2 \ln\left(1 - \left(\frac{r}{R_0}\right)^2\right), & (r \le R_0) \\ \infty \ , & (r > R_0) \end{cases} \tag{2}$$

$$U^{LJ}\left(r\right) = \begin{cases} 4\varepsilon\left[\left\{\left(\frac{\sigma}{r}\right)^{12} - \left(\frac{\sigma}{r}\right)^{6}\right\} - \left\{\left(\frac{\sigma}{r^{cut}}\right)^{12} - \left(\frac{\sigma}{r^{cut}}\right)^{6}\right\}\right], & \left(r \le r^{cut}\right) \\ 0 \ , & (r > r^{cut}) \end{cases} \tag{3}$$

where k is the spring constant, R_0 is the maximum extension of the spring, ε is the unit of the energy, σ is the unit of the length, and r^{cut} is the cutoff distance of the potential. The non-bonding interaction between the polymer segments separated by distance r is given by the Lennard-Jones potential $U^{LJ}(\mathrm{r})$. The parameters for the A and B beads will be described later.

Time evolution of the beads at position $\mathbf{r}_n$ is calculated by the Langevin equation,

$$m\frac{d^2\boldsymbol{r}_n}{dt^2} = -\frac{\partial U}{\partial \boldsymbol{r}_n} - \Gamma\frac{d\boldsymbol{r}_n}{dt} + \boldsymbol{W}_n(\mathrm{t}) \tag{4}$$

where m is the mass of the beads, U is the total potential energy of the system, and Γ is the friction constant. $\boldsymbol{W}_n(\mathrm{t})$ is the Gaussian white noise which is generated by the following equation.

$$\boldsymbol{W}_n(\mathrm{t})\boldsymbol{W}_m(\mathrm{t}') = 2k_BTm\Gamma\delta_{nm}\boldsymbol{I}\delta(t-t') \ . \tag{5}$$

We used the following parameter set: $k = 30.0\varepsilon/\sigma^2$, $R_0 = 3.0\sigma$, and $\Gamma = 0.5\tau^{-1}$, where τ is the unit of time. These parameters are the same as those of Grest and Kremer. The interval of one time step is 0.01τ, and the unit of temperature is $T_0 = k_B/\varepsilon$.

In this study, we focused on analysis of the structure of TPE. We used the simulation model and simulation conditions proposed by Aoyagi et al. [9]. For description of the hard and soft segments, the non-bonding interaction potential and temperature are controlled. To describe the hard domain by the A sub-chain, the attractive interaction potential (cutoff distance $r^{cut} = 2.5\sigma$) is imposed between A particles. Using this potential, aggregation of A particles, which is the spherical A domain, is derived. The temperature is also controlled and is set to $T = 0.4$ [T_0], which is less than the glass transition temperature of the melt polymer of A particles. Conversely, the B sub-chain is the model in a rubber state and the repulsive potential is set by using $r^{cut} = 1.12246\sigma$. The density of the particle is set to 0.85 σ^{-3}, and periodic boundary conditions are

applied in the x, y, and z directions for the cubic simulation box.

Construction of the initial structure is important to simulate the TPE of the ABA triblock copolymer. To realize the BCC sphere microphase separated structure by the ABA polymer, we used the node density biased Monte Carlo (NDBMC) method [9]. Here we will briefly describe the NDBMC method. First, a three-dimensional SCF simulation of the ABA block copolymer system is performed and the segment density $\phi(i, \mathbf{r})$ is obtained, where i and $\mathbf{r}$ are the segment number from one end and the position, respectively. A SCF simulation for A3B44A3 is performed. The parameters for the SCF simulation are $\chi = 2.4$ and system size = 32 x 32 x 32 with periodic boundary conditions. From the SCF simulation, the spherical domain structure described by the segment density, $\phi(i,\mathbf{r})$, is obtained. Using $\phi(i,\mathbf{r})$, a Monte Carlo simulation with the segment density weighted potential is performed to insert each bead of a polymer chain for CGMD and construct the initial structure. In the Monte Carlo simulation, the size of a single segment for SCF corresponds to two beads for CGMD. Note that the parameters for CGMD in the NDBMC simulation are the same values used in the following CGMD simulation. A relaxation simulation is then performed of 5.0×10^4 τ and the equilibrium structure with the BCC spherical domain is obtained.

Once the initial structure is obtained, a uniaxial elongation simulation is performed with a constant deformation rate of 0.00284436 σ/τ in the z direction. In each 100 steps, a small deformation of the simulation system with Poisson ratio 0.5 is applied. In this deformation, each bead moves under the condition of affine deformation, and the volume of the system is kept constant. In each interval of deformation, the polymer can relax, and deformation with chain relaxation is realized.

3. Results and discussions

3.1. Elongation simulation

The initial structure and the spherical domains of the A component ordered in the BCC sphere positions are shown in Fig. 2(a). In this structure, there are loop and bridge chains, and examples of these chains are shown in Fig. 2(b) and (c). Using this initial structure, we performed a uniaxial elongation simulation.

Snapshots during the elongation simulation are shown in Fig. 3. In this figure, only the interfaces of the A domain, whose density is 0.4 [σ^{-3}], are shown. From the initial structure (Fig. 3(a)) to the structure at strain of 2.0 (Fig. 3 (b)), the domains coalesce. From strain of 2.0 (Fig. 3 (b)) to strain of 4.0 (Fig. 3(c)), domain breaking and coalescence occur. To quantitatively analyze the structures, we estimated the number of domains and bridge fraction at each strain, and they are shown in Fig. 4 (a). As the strain increases, the number of domains decreases until strain of 2.0. When the strain becomes larger than 2.0, the number of domains increases. The bridge fraction decreases until strain of 3.0, and it then increases for larger strain. The stress-strain curve obtained by the CGMD simulation is shown in Fig. 4(b). The gradient decreases at strain of 3.0. These features are almost the same as a previous study [9], because the simulation conditions, including the block ratio, were the same and the simulation can be replicated.

Using the simulation results, the structural changes of the domains in the expansion process were analyzed. Collapse and breaking are phenomena derived from conformational change of the triblock copolymer. Therefore, by determining the domains that belong to each A sub-chain, the trace of each domain at each strain can be analyzed. A schematic diagram of the transition of the domains at each strain (γ) is shown in Fig. 5. The spheres show the domains at each strain, and the connected lines between two domains at different strains indicate the historical relation between the domains. For example, the 5th domain at strain of 1.5 originates from the 10th domain at strain of 1.0. Because the 1st domain at $\gamma = 1.5$ originates from the 1st, 2nd and 3rd domains at $\gamma = 1.0$, domain collapse occurs. The 2nd, 4th, and 5th domains at $\gamma = 3.0$ are related to the 3rd domain at $\gamma = 2.5$, which breaks into three domains. By these analyses, the changes of the domains can be understood.

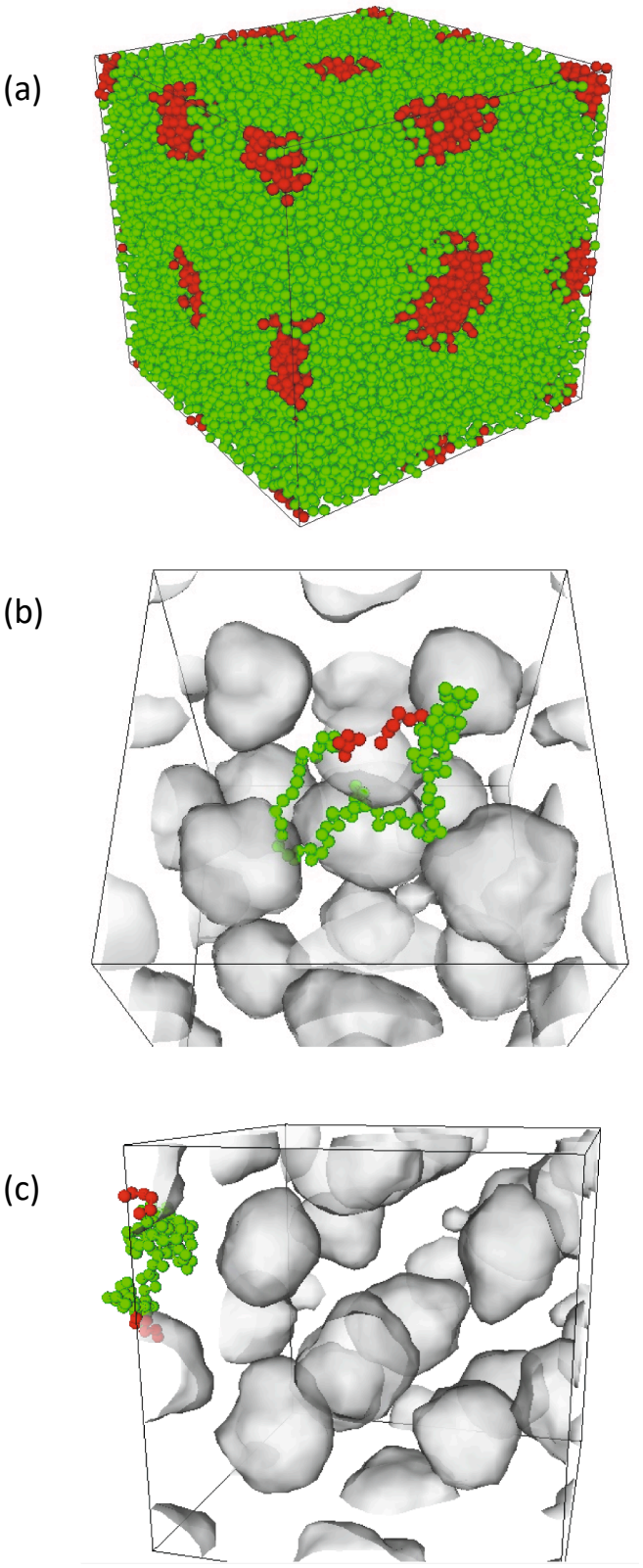

Fig. 2. (a)Snapshot of the initial structure of the spherical domain and examples of (b) bridge and (c) loop chains in the domain structure.

In the strain range 0.0–2.0, many domains collapse, and the number of domains decreases. Conversely, in the strain range 2.0–5.0, both domain collapse and breaking occur, and, as a result, the number of domains increases. This simultaneous event can only be observed by analysis of

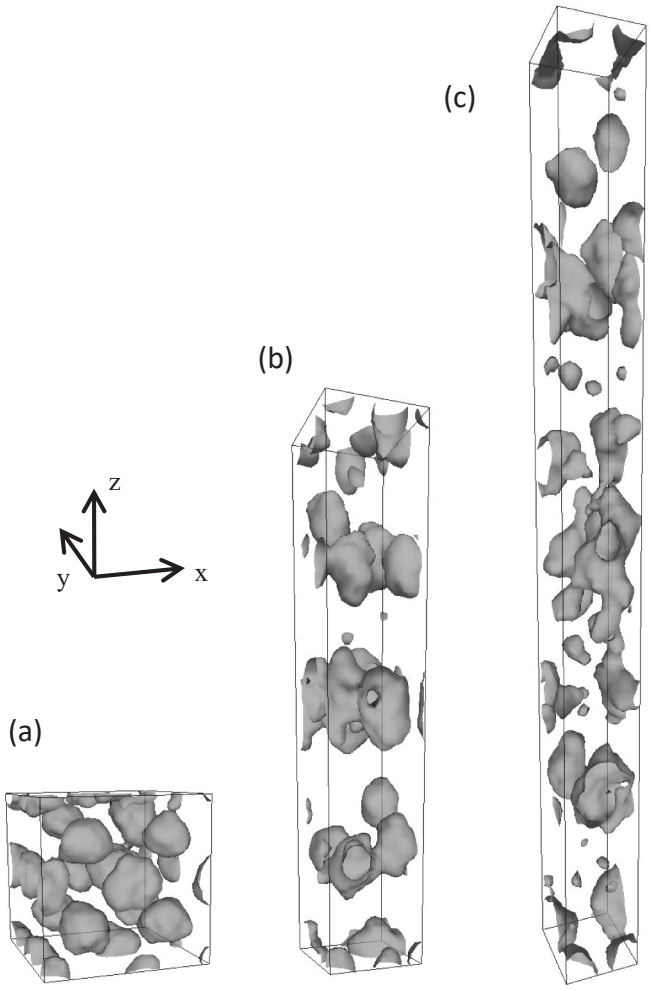

Fig. 3. Snapshots of the interfacial structure in the expansion simulation at strain of (a) 0.0, (b) 2.0, and (c) 4.0.

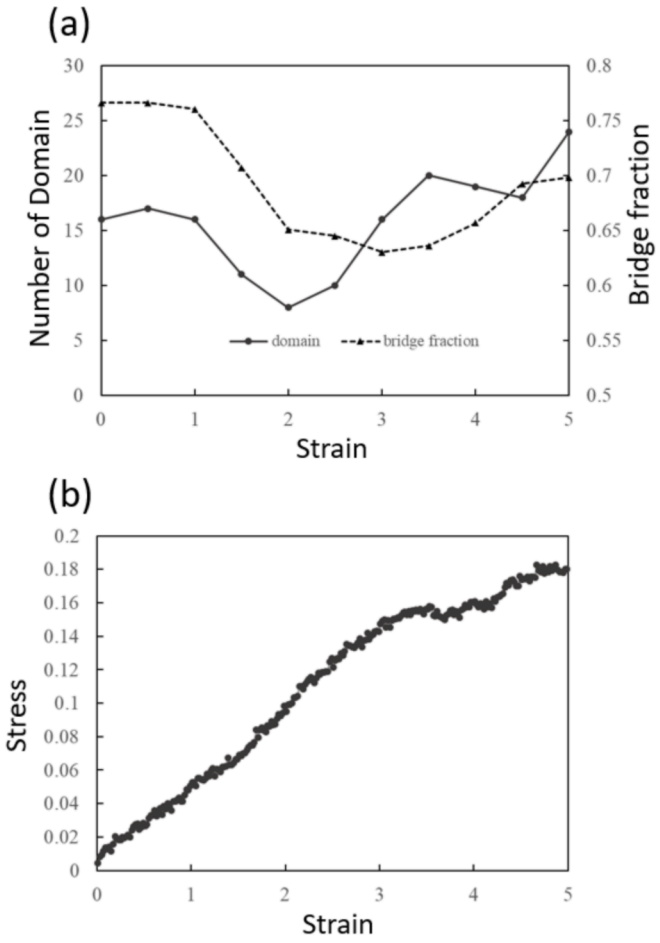

Fig. 4. Simulation results of the (a) the changes of the fraction of bridge chains and number of domains, and (b) stress-strain curve.

the conformation of each polymer.

3.2. Graphs of the elongation simulation results

In section 3.1, we discussed the change of the domains along with the strain by precise analysis of the polymer conformation. Next, we propose the description of the connectivity of the domains by bridge chains at each strain. To express the connectivity of the domains by bridge chains, we used graph theory, which can be used to analyze networks appeared in various situations such as social networks, transportation networks, neural networks etc. [22,23]. The graph structure for the bridge chain networks in TPE is shown in Fig. 6. The eight-domain system shown in Fig. 6(a) is chosen as an example, and its graph is shown in Fig. 6(b). A node drawn by a circle indicates a domain in TPE, and a connected line, which is called an edge, indicates a connected bridge chain in TPE. If there are one or more connected bridge chains, a connected line is drawn so that existence of bridge chains is recognized. For example, a bridge chain exists between the 1st and 3rd domain in Figs. 6(a), 1st and 3rd circles are connected by edges in Fig. 6(b). The graph structure will describe the topology of bridge chain network and using this descriptor we can understand the changes in the elongation process.

Using this definition, the domain network composed of all of the bridge chains in the initial structure for the CGMD simulation is shown in Fig. 7(a). The original domain structure with the domain numbers is shown in Fig. 7(b). In this structure, there are 16 domains, and these domains are connected by several bridge chains. Because periodic boundary conditions are applied in the CGMD simulation, the 13th, 14th, 15th, and 16th domains become neighbors of the 1st, 2nd, 3rd, and 4th domains, and the circular-type graph shown in Fig. 7(a) is applied. Here we focus on the 9th domain, which is located at the center of the simulation box. In Fig. 7(a), the 9th domain is joined to the 3rd, 4th, 5th, 6th, 7th, 8th, 10th, 11th, 12th, 13th, 14th, 15th, and 16th domains. Among these domains, the 5th, 6th, 7th, 8th, 13th, 14th, 15th, and 16th domains are the nearest neighbor domains of the 9th domain, the 3rd, 10th, and 12th domains are the next nearest neighbor domains, and the 4th and 11th domains are the second next nearest neighbor domains. It can be easily determined that most of the bridge chains are classified as connected chains between nearest or next nearest domains. Because most of the domains are connected by bridge chains, it is almost a perfect graph, in which all of the edges are joined.

Next, we will discuss the graphs for other strains. As shown in Fig. 5, there are only eight domains at $\gamma = 2.0$, which is less than the number of domains in the initial structure because of coalescence of domains. This number can be easily determined from the graph shown in Fig. 8(a). From the viewpoint of the connectivity, most of the domains remain connected in the deformation process. At $\gamma = 3.0$ (Fig. 8(b)) and 4.0 (Fig. 8(c)), the number of domains increases, and the defects of the edges increase. This originates from both breaking and coalescence of domains, which will be described in detail later. At $\gamma = 5.0$ (Fig. 8(d)), many of the domains are connected by bridge chains, although there are fewer lines than in the initial structure. In this graph, there are many unicursal ring (polygon) structures, which is confirmed by several lines. This feature means that the domain network is connected through the periodic boundary, which may affect the mechanical stress in the

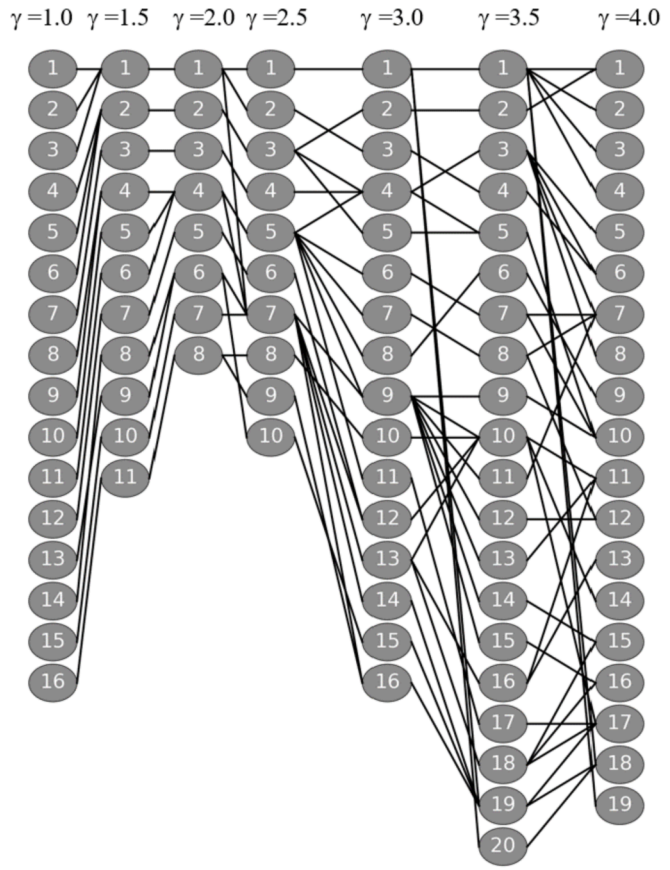

Fig. 5. Change of the domain structures at each strain (γ). The connected lines indicate the history of domains distinguished by the contained A sub-chains.

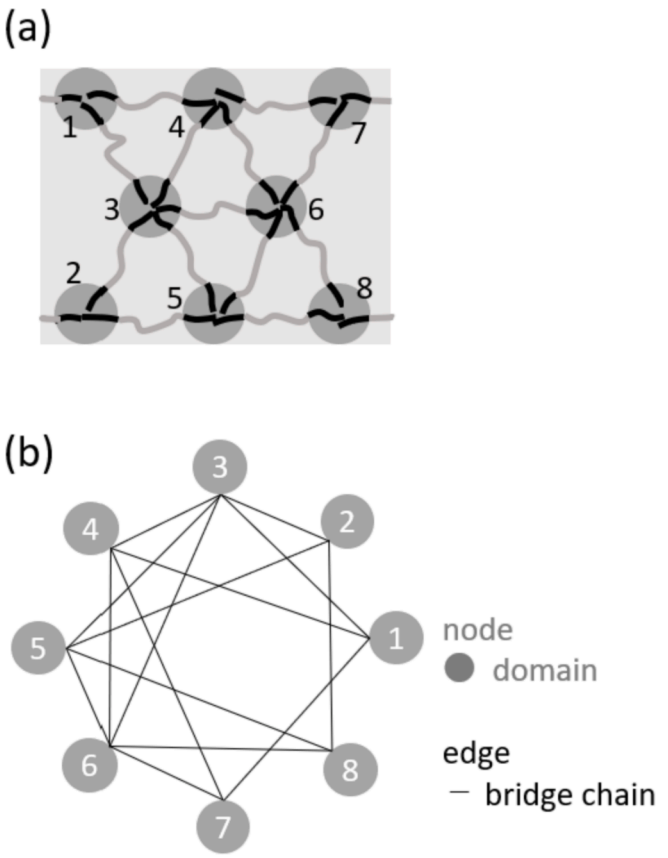

Fig. 6. Examples of (a) a domain structure and (b) its graph. The dark gray circles and light gray lines show the spherical domains and bridged chains, respectively.

deformation process.

3.3. Application of graph theory to analyze domain breaking and coalescence

As an application of graph theory, we show the analysis of the breaking and coalescence of domains using graphs. Focusing on a chain, snapshots and graphs of these processes are shown in Fig. 9. In Fig. 9(a) the domain structure at γ = 2.5 is shown with the bridge chain between the 1st and 5th domains. Its graph is shown in Fig. 9(d), where the specific bridge chain is indicated by a dashed line. If the strain increases to γ = 2.6, the right domain breaks into the 5th and 6th domains. At γ = 2.6, the same chain bridges the 1st and 5th domains (Fig. 9(b)), and its graph is indicated by a dashed line in Fig. 9(e). At γ = 2.6, the 5th domain is only connected to the 1st domain and the elongated bridge chain becomes unstable. To maintain the elongated chain structure, both A sub-chains must be pinned by the interfacial force originating from the attractive interaction between other A sub-chains within the A domain. However, the right part of A of the chain is released from the pinned force. Therefore, the chain shrinks, and the right part of the A sub-chain wants to join to another A domain. The domain structure at γ = 3.0 is shown in Fig. 9(c). The right domain coalesces with another domain and forms the 4th domain. As a result, the right A sub-chain belongs to the 4th domain at γ = 3.0. This result indicates that free-end-like domains, such as the 5th domain at γ = 2.6, are unstable and they are transient structures in the breaking and coalescence of domains. In the graphs shown in Fig. 9(d)–(f), the change of the domain structure and recombination of the bridge chain can be described.

In the graphs shown in Fig. 8 (b) and 8 (c), and 8 (d), there are many free-end-like domains and those are formed by the similar mechanism of domain breaking shown in Fig. 9. In Fig. 8(c) at γ = 3.0, 2nd, 3rd, 5th,

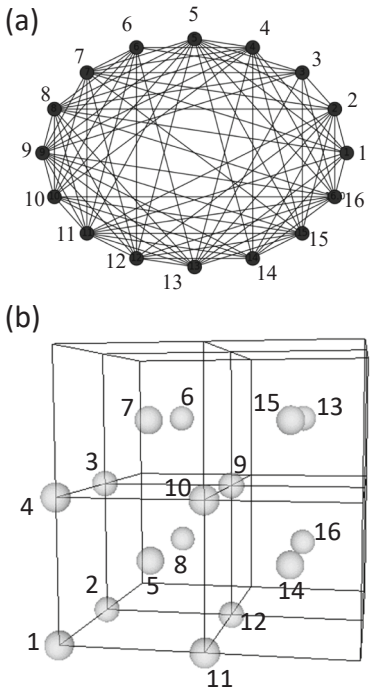

Fig. 7. (a) Graph of the initial structure and (b) the original domain structure.

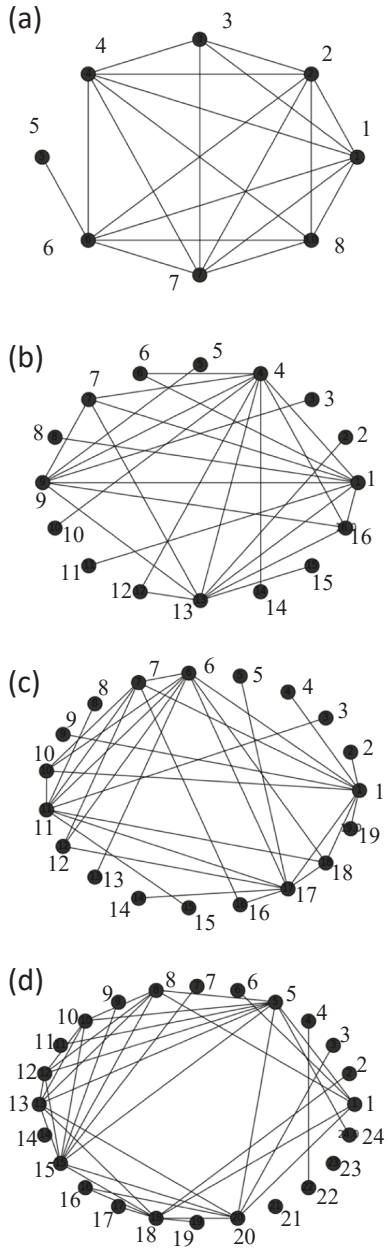

Fig. 8. Graphs for strain of (a) 2.0, (b) 3.0, (c) 4.0, and (d) 5.0.

8th, 10th,11th, 14th, and 15th domains are free-end-like domains. The background of each domain can be tracked back by Fig. 5. Within those domains, 2nd, 5th, 8th, 11th, and 14th domains are formed by the domain breaking in the deformation from $\gamma = 2.5$ to $\gamma = 3.0$, and 3rd, 10th, 15th domains are derived from $\gamma = 2.0$ to $\gamma = 2.5$. Detail changes of domains along the deformation can be traced by graphs combined with Fig. 5.

By a type of domain breaking shown in Fig. 9, per one time of domain breaking, both only one domain and only one bridge chain increase. Within the strain from 2.0 to 3.5, number of domains increases and many of the increased domains are made by a similar domain breaking shown in Fig. 9. Although number of domains increases in those strain range, number of bridge chains decreases as shown in Fig. 4. This is due to the coalescence of domain occurred with the same range. For example, from Fig. 5, 6th and 7th domains at $\gamma = 2.0$ coalesce to 7th domain at $\gamma = 2.5$. 3rd and 4th domains or 6th and 7th domains at $\gamma = 2.5$ coalesce to 4th and 12th domains, respectively. The contributed domains in those coalescences are larger domains. Once coalescence

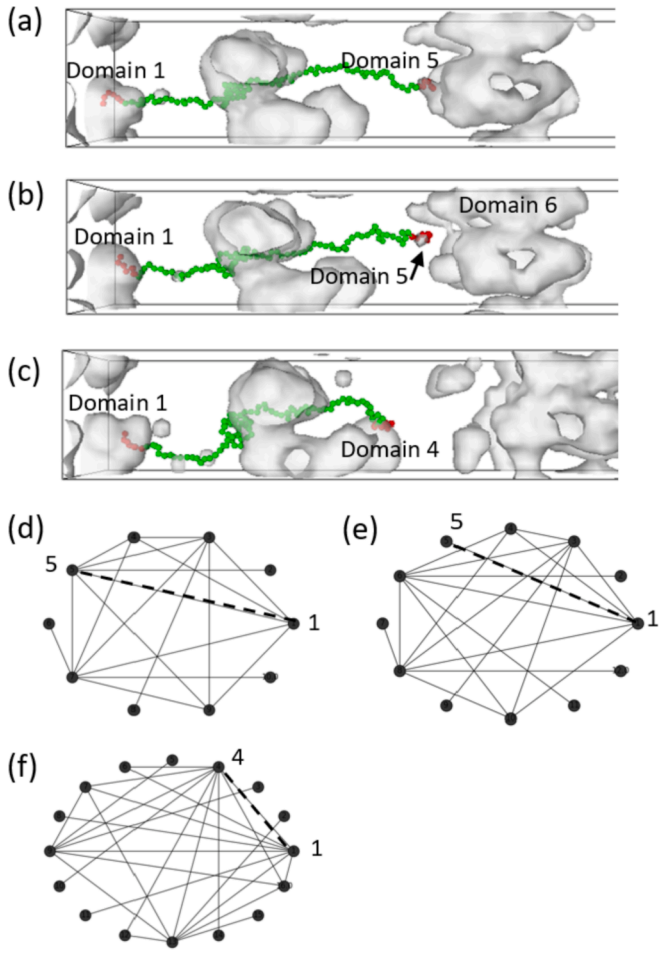

Fig. 9. Snapshots and graphs of breaking and coalescence of domains. (a)–(c) show the snapshot of the chains of interest and (d)–(f) show graphs at strain of 2.5, 2.6, and 3.0. Dashed lines in (d)–(f) indicate the polymer chains shown in Fig. (a)–(c), respectively.

occurs, many bridge chains change to loop chains, and bridge fraction decreases. By an analysis combined with Figs. 5 and 8, the changes of both number of domains and bridge fraction along the strain can be explained.

3.4. Correlation analysis among the physical quantities obtained by graph theory

To represent the adequacy and usefulness of the graph as a descriptor, we analyzed the physical quantities obtained by graph theory, which may become the numerical descriptor of the structure based on graph theory. Several physical quantities can be calculated from the graph, and we choose three following parameters, number of triangles, transitivity, and clustering coefficient. Once a graph was drawn, many triangles are formed by edge lines, and the number of triangles is the total number of triangles constituted by edges. The number of triangles depends on the diversity of the bridge chain and entropy of the system. As the strain increases during expansion, the number of triangles decreases, which may be related to expansion of the polymer chains. The transitivity is defined as the parameter which is a number of triangles divided by total number of triangles of the perfect graph by total nodes. The transitivity can be understood as the perfectivity of the graph and the inhomogeneity of the expanded structure can be understood from the change of the transitivity. Though the local clustering coefficient is defined as the ratio between the number of existing edges within the neighborhood of a node and the number of possible edges within the

neighborhood of a node at the focused node, the averaged clustering coefficient is averaged value of local clustering coefficients. The averaged clustering coefficient is the index of a small network or ring. The decrease of this value in the expansion process may be related to the decrease in the number of small triangles. The number of triangles, transitivity, and clustering coefficient are given in Table 1.

The correlation between these physical quantities can be represented by scatter diagrams, which are shown in Fig. 10. In these diagrams, the strain, stress, number of domains, and number of bridge chains are also taken as parameters. Several linear relations can be found in Fig. 10. Among the number of domains, number of triangles, and number of bridge chains, there are two types of linear relations in each figure: low and high gradient lines. For the scatter diagram between the number of domains and number of triangles, the low and high gradient lines indicated by the two arrows correspond to the data for strain below and above about 2.2, respectively. This result indicates that the mechanism of deformation at the level of the polymer chain and domain structures switches at about strain of 2.2. In Fig. 4(a), the number of domains starts to increase at about strain of 2.2 and domain breaking (i.e., domain fracture) occurs. In a previous study [9], a compression simulation was performed until $\gamma = 0$ from the expanded structure in which domain breaking occurs and the obtained structure at $\gamma = 0$ did not recover to the initial structure. We speculate that the two linear relations may correspond to the recoverably and destructively deformed states.

To verify the recoverably or destructively deformed structures in the elongation simulation results, we performed a compression simulation until $\gamma = 0$ from each elongated structure and counted the number of domains at $\gamma = 0$ to compare with 16 domains in the initial structure. In other words, we performed elongation-compression cycle simulations for different maximum strains and counted the number of domains after cycle simulation. Fig. 11 shows the number of domains after the compression simulation from each elongated structure. Horizontal axis indicates the strain at the start point of compression simulation. For compression from the elongated structures of less than or equal to 2.0 strain, the number of domains is about 16, which is almost same as the number of domains of the initial structure. This indicates that the domain structure is almost recovered after the elongation-compression cycle simulation. In contrast, for compression from the elongated structures of greater than 2.0 strain, the number of domains is less than 16 and the domain structure is not recovered after the cycle simulation. For compression from the elongated structure of large strain, domain coalescence occurs in the compression process and reconfiguration of broken domains and bridge chains occurs. From these compression simulations, the boundary between recoverable and destructive deformation is the same as the transition point of the strain between the two lines shown in Fig. 10. We also performed simulations using other initial structures. The same results were obtained, although the boundary strains were fluctuated. From these results, the fractured domain structure can be confirmed using the correlation among the number of domains, number of triangles, and number of bridge chains, and the quantities obtained from the graph theory can be used as an indicator of fracture inside the TPE.

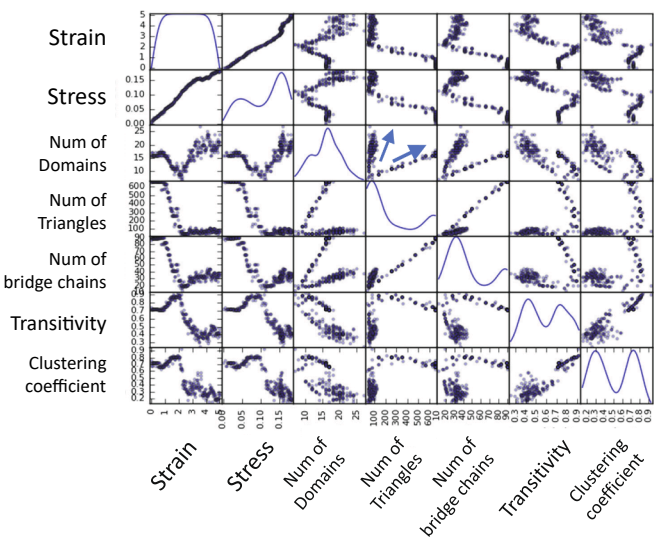

Fig. 10. Scatter diagrams among the physical quantities strain, stress, number of domains, number of triangles, number of bridge chains, transitivity, and clustering coefficient. The diagonal figures are histogram along the horizontal axis.

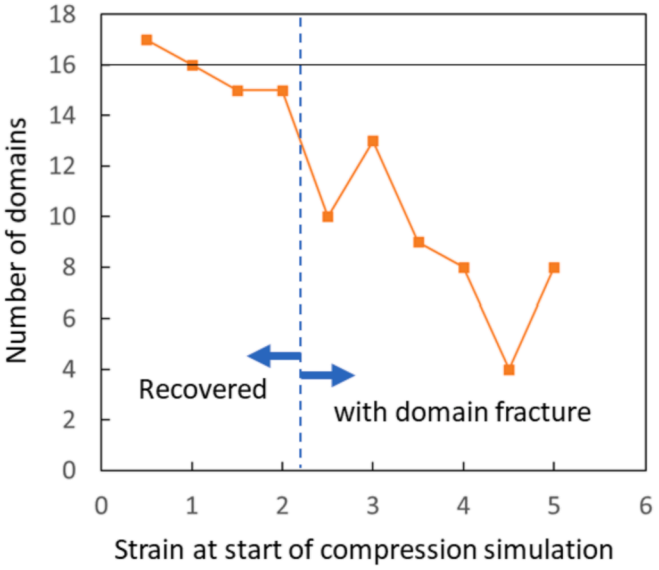

Fig. 11. Comparison between the number of domains after one cycle of the elongation–compression simulation and the initial structure. The horizontal line at 16 is the number of domains in the initial structure.

4. Conclusion

Graph theory including information about both the domain and bridge chain network structures composed of the ABA block copolymer is applied to analyze the deformed domain structure during elongation of TPE. Using this analysis, the structures of the domain and the bridge chain network can be simply described and the changes of the number of domains and recombination of the network, such as breaking and coalescence of domains, in the deformation process can be easily found. This is an important description method for many-chain systems in microphase separated structures, and it can also be applied to other types of structures, such as lamellar and cylindrical phase separated structures. Once the graph is obtained, the graph itself and the physical

Table 1
Number of triangles, transitivity, and average clustering coefficient calculated from the graph at each strain.

Strain	0	0.5	1	1.5	2	2.5	3	3.5	4	4.5	5
Number of Triangle	657	657	630	255	78	48	54	54	48	75	90
Transitivity	0.718	0.710	0.753	0.870	0.857	0.658	0.425	0.316	0.318	0.441	0.479
Average_clustering coefficient	0.719	0.670	0.709	0.802	0.767	0.453	0.341	0.386	0.198	0.290	0.252

quantities determined from the graph can be treated as the parameters to describe the structure of TPE and the topology of bridge chain network, which cannot be found by usual analysis. It is derived that the two types of deformation state in the deformation process can be analyzed. In the future, we will apply this method to analyze the fractured structures of other microphase separated structures.

Author contributions

The manuscript was written through contributions of all authors. Computation and analysis are mainly performed by H. M. and A. M. and these results are approved by all authors. All authors have given approval to the manuscript.

Declaration of competing interest

The authors declare that they have no known competing financial interests or personal relationships that could have appeared to influence the work reported in this paper.

Acknowledgements

This work is supported by JST CREST Grant Number JPMJCR17J4, Japan.

References

[1] G. Holden, N.R. Legge, R.P. Quirk (Eds.), Thermoplastic Elastomers, Hanser Gardner, New York, 1996.
[2] G.H. Fredrickson, F.S. Bates, Dynamics of block copolymers: theory and experiment, Annu. Rev. Mater. Sci. 26 (1996) 501.
[3] G. Fredrickson, The Equilibrium Theory of Inhomogeneous Polymers, Oxford University Press, Oxford, 2005.
[4] M.W. Matsen, M. Schick, Lamellar phase of a symmetric triblock copolymer, Macromolecules 27 (1994) 187.
[5] H. Watanabe, Slow dielectric relaxation of a styrene-isoprene-styrene triblock copolymer with dipole inversion in the middle block: a challenge to a loop/bridge problem, Macromolecules 28 (1985) 5006.
[6] H. Watanabe, T. Sato, K. Osaki, M.-L. Yao, A. Yamagishi, Rheological and dielectric behavior of a styrene– isoprene– styrene triblock copolymer in selective solvents. 2. contribution of loop-type middle blocks to elasticity and plasticity, Macromolecules 30 (1997) 5877.
[7] K. Karatasos, S.H. Anastasiadis, T. Pakula, H. Watanabe, On the loops-to-bridges ratio in ordered triblock copolymers: an investigation by dielectric relaxation spectroscopy and computer simulations, Macromolecules 33 (2000) 523.
[8] J. Huh, W.H. Jo, G. ten Brike, Conformational analysis in ABA triblock melts by Monte Carlo simulation, Macromolecules 35 (2002) 2413.
[9] T. Aoyagi, T. Honda, M. Doi, Microstructural study of mechanical properties of the ABA triblock copolymer using self-consistent field and molecular dynamics, J. Chem. Phys. 117 (2002) 8153.
[10] M.W. Matsen, R.B. Thompson, Equilibrium behavior of symmetric ABA triblock copolymer melts, J. Chem. Phys. 111 (1999) 7139.
[11] F. Drolet, G.H. Fredrickson, Optimizing chain bridging in complex block copolymers, Macromolecules 34 (2001) 5317.
[12] Z. Wang, B. Li, Q. Jin, D. Ding, A.C. Shi, Simulated annealing study of self-assembly of symmetric ABA triblock copolymers confined in cylindrical nanopores, Macromol. Theory Simul. 17 (2008) 86.
[13] E. Helfand, Z.R. Wasserman, Block copolymer theory. 4. Narrow interphase approximation, Macromolecules 9 (1976) 879.
[14] G.J. Fleer, M.A. Cohen Stuart, J.M.H.M. Scheutjens, T. Cosgrove, B. Vincent, Polymers at Interfaces, Chapman & Hall, London, 1993.
[15] M.W. Matsen, M. Schick, Stable and unstable phases of a diblock copolymer melt, Phys. Rev. Lett. 72 (1994) 2660.
[16] M. Hatakeyama, R. Faller, Coarse-grained simulations of ABA amphiphilic triblock copolymer solutions in thin films, Phys. Chem. Chem. Phys. 9 (2007) 4662.
[17] A.J. Parker, J. Rottler, Molecular mechanisms of plastic deformation in sphere-forming thermoplastic elastomers, Macromolecules 48 (2015) 8253.
[18] A.J. Parker, J. Rottler, Nonlinear mechanics of triblock copolymer elastomers: from molecular simulations to network models, ACS Macro Lett. 6 (2017) 786.
[19] K. Kremer, G.S. Grest, Dynamics of entangled linear polymer melts: a molecular-dynamics simulation, J. Chem. Phys. 92 (1990) 5057.
[20] S.S. Tallury, K.P. Mineart, S. Woloszczuk, D.N. Williams, R.B. Thompson, M. A. Pasquinelli, M. Banaszak, R.J. Spontak, Molecular-level insights into asymmetric triblock copolymers: network and phase development, J. Chem. Phys. 141 (2014) 121103.
[21] T. Aoyagi, F. Sawa, T. Shoji, H. Fukunaga, J. Takimoto, M. Doi, A general-purpose coarse-grained molecular dynamics program, Comput. Phys. Commun. 145 (2002) 267.
[22] R. Diestel, Graph Theory, fifth ed., Graduate Texts in Mathematics, Springer, 2017.
[23] D. Watts, S. Strogatz, Collective dynamics of 'small-world' networks, Nature 393 (1998) 440.
[24] Y. Tezuka (Ed.), Topological Polymer Chemistry: Progress of Cyclic Polymers in Syntheses, Properties and Functions, World Scientific, Singapore, 2013.
[25] Y. Tezuka, Topological polymer chemistry designing complex macromolecular graph constructions, Acc. Chem. Res. 50 (2017) 2661.